Ordering phenomena of star polymer solutions approaching the Θ state

C. N. Likos,[1] H. Löwen,[1,2] A. Poppe,[3] L. Willner,[3] J. Roovers,[4] B. Cubitt,[5] and D. Richter[3]
[1]*IFF Theorie II, Forschungszentrum Jülich GmbH, D-52425 Jülich, Germany*
[2]*Institut für Theoretische Physik II, Heinrich-Heine-Universität Düsseldorf, Universitätsstraße 1, D-40225 Düsseldorf, Germany*
[3]*IFF Neutronenstreuung II, Forschungszentrum Jülich GmbH, D-52425 Jülich, Germany*
[4]*Institute for Environmental Chemistry, National Research Council of Canada, Ottawa, Ontario, Canada K1A 0R6*
[5]*Institute Laue-Langevin, 156 Avenue des Martyrs, F-38042 Grenoble, Cedex 9, France*
(Received 9 June 1998)

The liquid-state ordering phenomena of a semidilute polybutadiene 64-arm star polymer solution were investigated by small-angle neutron scattering. For this purpose, we used deuterated 1,4-dioxane, which is a Θ solvent for the star at 31.5 °C. Its quality was modified by varying the temperature in the range between 40 °C and 80 °C. Besides a swelling of the star, with increasing temperature the development of a strong correlation peak was observed in the experiment. The experimental data were described theoretically by employing an effective pair potential between stars which was introduced earlier by Mewis *et al.* [J. Mewis, W. J. Frith, T. A. Strivens, and W. B. Russel, AIChE J. **35**, 415 (1989)]. [S1063-651X(98)13611-5]

PACS number(s): 61.25.Hq, 61.12.−q, 61.20.Gy, 82.70.Dd

I. INTRODUCTION

Star polymers consist of f polymeric arms attached to a common center, which is negligibly small in comparison to the overall size of the molecule [1]. Because of their peculiar architecture, they can be viewed as hybrids between polymers and colloidal particles. Therefore an investigation of their static and dynamical properties is of great interest, experimentally as well as theoretically, as they provide a bridge between these two areas of condensed matter physics. From the experimental point of view, some of the relevant questions are the effect of the arm number (functionality) f, the degree of polymerization N, and the quality of the solvent on the properties of a single star and, more importantly, on the structure and ordering of concentrated solutions of star polymers.

For the theorist, the goal is to describe the solution by employing an effective interaction (preferably on the pair level) between the centers of the stars, which results, in principle, after the solvent as well as the polymeric degrees of freedom have been canonically traced out, thus leaving the star centers as the only remaining degrees of freedom (''point particles'') in the system. If that goal is achieved, then the whole machinery from liquid-state theory and standard statistical mechanics can be employed to describe quantitatively the structure and thermodynamics of the star solutions, including possible phase transformations. It is expected that the form of such a pair interaction will depend on the parameters mentioned above, i.e., f, N, and solvent quality.

In previous work [2] we studied a solution of 18-arm stars in a good solvent for a wide range of polymer concentration (or star density). By way of direct comparison with experimental data, it was demonstrated that stars in a good solvent can be quantitatively described if one employs an effective interaction consisting of a logarithmic term for short separations, as proposed by Witten and Pincus [3], combined with a Yukawa tail for larger distances. In order to investigate the effect of the quality of the solvent on the ordering of the stars, we now turn our attention to a semidilute solution of 64-arm stars in the vicinity of the Θ temperature. Again, by comparing with experiment, we find that a different pair potential has to be employed now, in particular the one which results from a Derjaguin approximation on the corresponding interaction between flat plates grafted with polymers in a solvent which induces weak excluded volume interactions. The latter was calculated earlier by Milner *et al.* [4].

The paper is organized as follows. In Sec. II we present details on the synthesis, preparation, and experimental procedure employed for the study of the stars and in Sec. III the results of the experiment. In Sec. IV we explain the theoretical approach and compare with the experimental results. Finally, in Sec. V we summarize and conclude.

II. EXPERIMENT

A. Synthesis and characterization of the star polymers

The star polymer under investigation was built of polybutadiene and contained 64 arms. The detailed synthesis is described elsewhere [5]. In a first step, a narrow molecular weight living polybutadiene was prepared using anionic polymerization techniques and *s*-BuLi as initiator. A small fraction of the polymer was removed and terminated with methanol. It was used as a reference material for the determination of the number of arms per star. The living polydiene was reacted with a 64-functional chlorosilane compound and the resulting star was fractionated extensively in a toluene-methanol mixture in order to remove excess arm material. All polymer solutions were protected against oxidation, degradation, and cross linking by 4-methyl-2,6-di-*tert*-butylphenol. The weight-average molecular weight of the star was determined by low-angle laser light scattering (LALLS) [6] to be 725 000 g/mol, the number-average molecular weight of the arm was 12 100 g/mol, yielding a number of arms per star of 60 and a degree of polymerization per arm $N_0 = 168$. The investigation by size exclusion chromatography (SEC) yielded a narrow distribution of molecular

 © 1998 The American Physical Society

weights, $M_W/M_n=1.01$, where M_W is the weight-average molecular weight and M_n the number-average molecular weight.

B. Sample preparation

For all solutions, fully deuterated 1,4-dioxane served as a solvent. For the measurements, solutions of two different concentration regimes were prepared. First, a dilution series of three dilute solutions was mixed in order to determine the form factor of the star. Thereby, star volume fractions of 0.0032, 0.0080, and 0.0127 were chosen. Additionally, a solution was prepared in order to investigate the ordering phenomena. Its volume fraction was 0.104, which is close to the overlap concentration. The value for the overlap concentration was estimated in advance using previous results [6].

The stock solution for the dilution series was generated by mixing the polymer and the solvent first and afterwards heating the mixture to 40 °C. Thereby, the polymer was dissolved completely. Turbidity measurements yielded a Θ temperature of 31.5 °C for this solvent. Therefore the dilution of the stock solution was performed in a heat bath at 40 °C.

Because of the expected high viscosity of the semidilute star polymer solution, the sample preparation was performed in two steps. First, a solution of the polymer in benzene was filled in a sample cell. Then, the solvent was removed by freeze-drying and, in a second step, an appropriate volume of 1,4 dioxane was added. The dissolution of the polymer was achieved by heating up to 40 °C. The sample cells were equipped with special seals and evaporated in order to avoid solvent losses during heating.

C. Small-angle neutron scattering (SANS)

The SANS experiments were performed at five different temperatures, 40 °C, 50 °C, 60 °C, 70 °C, and 80 °C. The accuracy of the temperature was 1 °C. Neglecting interparticle scattering contributions, the coherent macroscopic scattering cross section is of the general form

$$\frac{d\Sigma}{d\Omega}(Q)=\frac{\Delta\rho^2}{N_A}\phi V_W P(Q), \tag{2.1}$$

where V_W denotes the weight-average molar volume of the polymer, ϕ the volume fraction of the star, $\Delta\rho^2$ is the contrast factor between the solvent and the star, $P(Q)$ denotes the normalized form factor, and N_A the Avogadro number. The contrast factor $\Delta\rho^2$ was calculated from the scattering length densities ρ_i by $\Delta\rho=\rho_{\text{solvent}}-\rho_{\text{star}}$, where ρ_{solvent} refers to the scattering length density of the solvent and ρ_{star} to that of the star polymer. The scattering length densities were obtained using the equation

$$\rho_i=\frac{\Sigma b_z}{v_i}, \tag{2.2}$$

where b_z is the coherent scattering length of an individual atom z of the solvent molecule or the repeat unit of the polymer and v_i are the respective volumes. In order to account for the temperature dependence of the density and thus v_i of these compounds, the following relations were taken from the literature [7,8]:

$$\rho_{\text{dioxane}}=\rho^0_{\text{dioxane}}\exp[-8.5\times10^{-4}\times(T-T_0)], \tag{2.3}$$

with $T_0=25$ °C and $\rho^0_{\text{dioxane}}=1.13$ g/cm^3. For polybutadiene, the density exhibits a temperature dependence of

$$\rho_{\text{PB}}=\rho^0_{\text{PB}}\exp[-7.5\times10^{-4}\times(T-T_0)], \tag{2.4}$$

with $T_0=25$ °C and $\rho^0_{\text{PB}}=0.90$ g/cm^3. Besides the scattering length density, also the volume fractions were corrected for the change of the density with temperature.

The SANS experiments were carried out with the D17 diffractometer at the Institute Laue-Langevin in Grenoble. The solutions were studied in 2 mm quartz sample cells, yielding transmissions in the range between 0.6 and 0.85. Using a wavelength of 11.7 Å at a sample detector distance of 2.8 m, a Q range of 0.013 Å$^{-1}\leqslant Q\leqslant$0.13 Å^{-1} was covered. The raw data were corrected for different detector cell efficiencies and calibrated to absolute units by using water as a secondary standard [9] according to

$$\frac{d\Sigma}{d\Omega}(Q)=\frac{L^S h^S T^S M^S I_m(Q)}{LhTMI^S_m(0)}\left(\frac{d\Sigma(0)}{d\Omega}\right)^S. \tag{2.5}$$

Here S refers to the standard, M denotes the total monitor counts, h the sample thickness, L the sample to detector distance, and T the transmission. $I_m(Q)$ is the scattered intensity and $I^S_m(0)$ the measured intensity of the standard at $Q=0$. The value of $(d\Sigma(0)/d\Omega)^S$ for the water standard was calibrated with vanadium to be 0.99 cm^{-1}. Finally, the coherent differential cross section was obtained by subtracting the scattering contribution of the solvent as well as the incoherent contribution of the polymer.

III. RESULTS

A. Dilute solutions

The coherent differential cross sections were normalized to the polymer volume fraction and multiplied with the factor $N_A/\Delta\rho^2$. At low Q, the concentration-scaled scattering curves reveal differences due to intermolecular contributions. In order to eliminate such effects, the data were extrapolated to infinite dilution, applying the Berry-extrapolation method [10]. Due to the limited Q range the usual Zimm extrapolation could not be employed meaningfully. In the limit $\phi\rightarrow0$ the cross section reveals the single star form factor $P(Q)$:

$$\frac{N_A}{\Delta\rho^2}\frac{1}{\phi}\frac{d\Sigma}{d\Omega}(Q,\phi\rightarrow0)=V_W P(Q). \tag{3.1}$$

From the extrapolation at low Q the second virial coefficient A_2 and the radius of gyration R_G are obtained. The molecular volume was kept as a fixed parameter, since it was determined separately by static light scattering. It varies slowly following the temperature dependence of the density given by Eq. (2.4). Table I presents the results for the temperatures under investigation. In Fig. 1 A_2 is shown as a function of temperature. Extrapolating the two points at the lowest temperatures by a straight line, the Θ temperature T_Θ is determined to 31 °C. In accordance with this result, turbidity measurements revealed $T_\Theta=31.5$ °C.

TABLE I. Results of the Berry extrapolation.

T (°C)	A_2 (10^{-4} ml mol g^{-2})	R_G (Å)	V_W (10^3 cm^3 mol^{-1})
40	0.16±0.04	114±8	819
50	0.32±0.07	124±8	821
60	0.37±0.09	132±9	827
70	0.40±0.09	136±9	833
80	0.44±0.09	141±9	839

In Fig. 2 we show the temperature-dependent swelling of the radius of gyration on a double logarithmic scale. In order to prove the scaling behavior of the stars, the data of the highest four temperatures were described by a straight line with the slope of 1/8. The value of 1/8 originates from the scaling laws proposed by Daoud and Jannink [11] for solutions of linear polymers. In this model the scaling behavior of polymer solutions depends on the reduced temperature $\tau=(T-T_\Theta)/T_\Theta$ and the polymer volume fraction ϕ. Thereby, T and T_Θ denote the absolute temperature and the Θ temperature in degrees Kelvin. Close to the Θ temperature, the radius of gyration is predicted to be independent of τ, while at higher temperatures and in the case of semidilute solutions, it should scale as

$$R_G \sim \tau^{1/8}. \tag{3.2}$$

The assumption of a semidilute solution is justified, since the density of the chains in the star is rather high and thus resembles a semidilute solution of linear chains. The excellent agreement with the experimental data supports the validity of the theory. For the lowest temperature, we guess that the τ-independent scaling regime is reached.

At higher Q the particularities of the form factor $P(Q)$ come into play. In order to parametrize $P(Q)$ over a large Q range we invoked the scattering cross section from polymeric mass fractals, developed by Beaucage [12,13]. In the simplest case, this form factor contains two contributions:

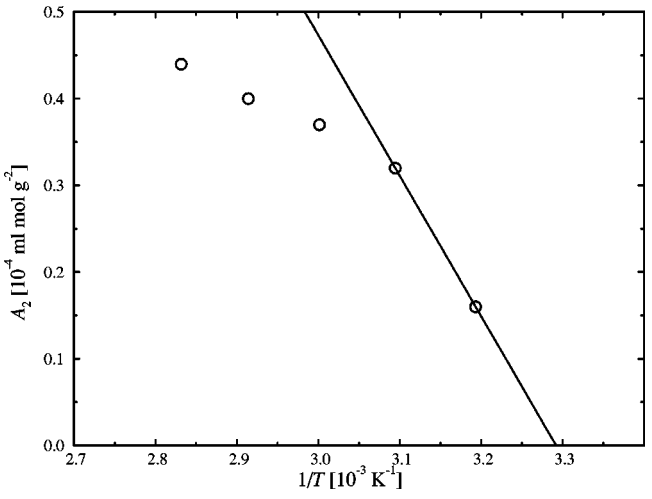

FIG. 1. Second virial coefficients plotted vs the inverse temperature. The solid line represents a linear fit to the data points of the lowest temperature. Thereby, a Θ temperature of 31 °C was obtained.

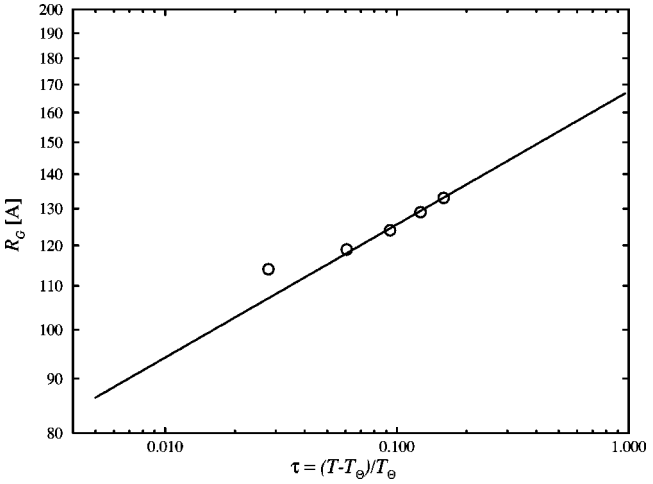

FIG. 2. Double logarithmic plot of the radius of gyration R_G of the stars against the reduced temperature $\tau=(T-T_\Theta)/T_\Theta$, where T is the absolute temperature. The straight line has slope 1/8.

$$V_W P(Q) = V_W \exp(-Q^2 R_G^2/3) + B\left(\frac{[\mathrm{erf}(1.06 Q R_G/\sqrt{6})]^3}{Q}\right)^{d_f} \equiv G(Q)+F(Q). \tag{3.3}$$

The first term, $G(Q)$, contributes in the low Q range and describes the overall size of the object. It is written in the form of a Guinier function. The second, $F(Q)$, is substantial at high Q values and reflects the short range, i.e., monomer correlations. In Eq. (3.3), V_W denotes the weight-average molecular volume, R_G the radius of gyration, and d_f the dimension of the polymeric mass fractal. The quantity B is the prefactor of the power law term. It is defined according to the regime in which the exponent d_f falls and reads [12,13]

$$B = \left(\frac{V_W d_f}{R_G^{d_f}}\right)\Gamma\left(\frac{d_f}{2}\right), \tag{3.4}$$

where Γ denotes the gamma function. Thus, using Eq. (3.4), the expression for the form factor is constrained and only three unknowns, i.e., V_W, R_G, and d_f, remain as fit parameters. Since our interest in this context is to describe the experimental form factor as accurately as possible by a theoretical expression, the parameters d_f, R_G, and B were treated as adjustable. Also V_W was an adjustable parameter at 40 °C. At higher temperature its value was adjusted following the density change according to Eq. (2.4). Instrumental resolution effects were taken into account by a Gaussian-type resolution function [14], given by

$$R(Q,Q_0) = \frac{1}{\sqrt{2\pi}\Delta Q}\exp\left[-\frac{1}{2}\frac{(Q-Q_0)^2}{(\Delta Q)^2}\right], \tag{3.5}$$

where Q_0 is the considered scattering vector, $(\Delta Q)^2 = (2\pi\Delta\theta/\lambda)^2 + (Q_0\Delta\lambda/\lambda)^2$, with $\Delta\theta = 4.6\times10^{-3}$ being the uncertainty in the scattering angle and $\Delta\lambda/\lambda = 0.051$ the relative uncertainty of the wavelength. For the fit, the resolution function was convoluted with the theoretical form factor. The results of these fits are shown in Fig. 3 and listed in Table II. Excellent agreement between experiment and the

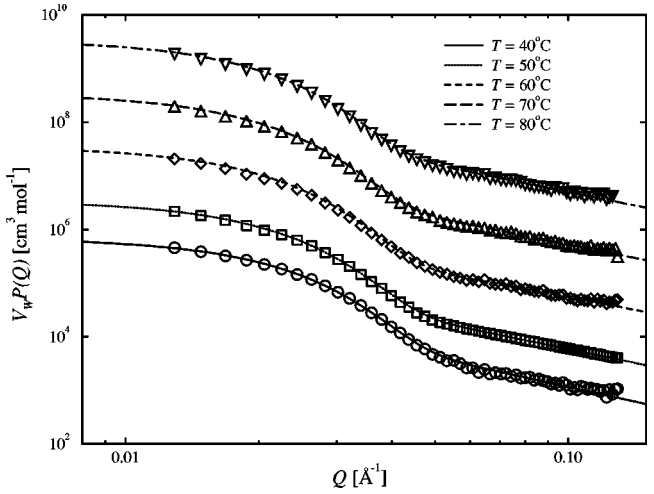

FIG. 3. Form factors of the star at 40 °C, 50 °C, 60 °C, 70 °C, and 80 °C. The solid lines represent the fits according to the Beaucage model. For the sake of clarity the data were multiplied by constants: 50 °C:5, 60 °C:50, 70 °C:500, 80 °C:5000.

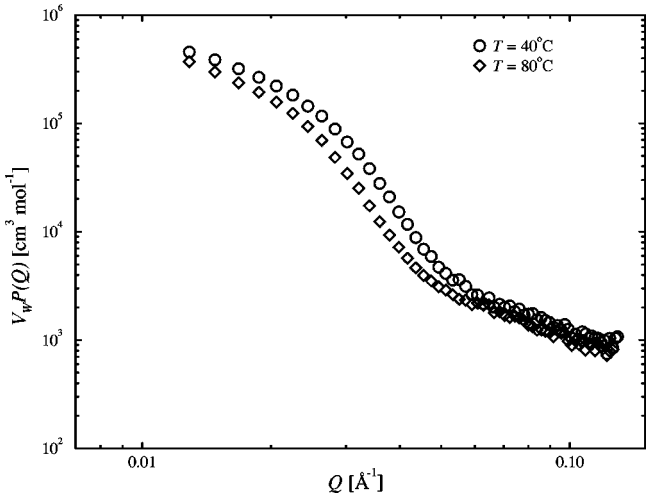

FIG. 4. The form factors at 40 °C and 80 °C. The decrease in intensity at different Q values is due to the swelling of the stars.

functional form of Eq. (3.3) is obtained for all temperatures under investigation. We note that the description with the Beaucage formalism was undertaken in order to obtain a good parametrization of the data. Table II shows that thereby, e.g., the molecular volumes come out too low as well as the radii of gyration come out lower than in the model-independent Berry extrapolation and the light-scattering data. This fact points to deficiencies of the Beaucage formula which if compared with analytical star form factors like the one by Benoit for Gaussian stars [15] displays discrepancies already in the first correction to the Guinier approximation. For the purpose of accurate parametrization this is of no significance. In order to show the effect of star swelling the experimental form factors at 40 °C and 80 °C are compared in Fig. 4.

B. At the overlap concentration

While the data from the dilute solutions are dominated by the single star form factor, close to the overlap concentration the interstar structure factor $S(Q)$ strongly influences the scattering behavior. In this concentration range the absolute cross section for the nearly monodisperse stars is approximated by

$$\frac{d\Sigma}{d\Omega}(Q)=\frac{\Delta\rho^2}{N_A}\phi[G(Q)S(Q)+F(Q)]. \tag{3.6}$$

TABLE II. Results of the Beaucage fits.

T (°C)	R_G (Å)	V_W (10^3 cm^3 mol^{-1})	B (10^{15} cm$^{3-d_f}$ mol^{-1})	d_f
40	91	707	7.51	1.83
50	95	712	0.84	1.71
60	98	717	0.28	1.63
70	101	723	0.12	1.58
80	103	728	0.08	1.56

This factorization ansatz considers the two contributions to the form factor in a qualitatively different way. (i) $G(Q)$, describing the overall shape, is an approximation to the overall density of the star. Scattering from different stars is able to interfere—therefore $G(Q)$ is associated with $S(Q)$. (ii) $F(Q)$ originates from local correlations and can be considered as diffuse scattering. Such regions of diffuse scattering are uncorrelated as in the case of incoherent scattering. Interferences do not take place. Therefore $F(Q)$ is not modified by $S(Q)$. The shape of the stars was determined in dilute solution. Here we assume that it does not change with concentration. Experimentally [16] it has been shown for 64-arm stars in a good solvent that no deformation occurs in a regime up to the overlap concentration. The overlap concentration is the concentration at which the stars begin to interpenetrate each other. It is given by

$$\phi^*=3V_W(4\pi R_G^3 N_A)^{-1}. \tag{3.7}$$

In order to prove the validity of Eq. (3.6), the values for the overlap concentration were calculated for all temperatures under investigation employing the results of SANS (Table II) for R_G. Values of 0.14 at 80 °C up to 0.22 at 40 °C were found. The decrease of ϕ^* with increasing temperature is due to the swelling of the star, but this effect is not strong enough to affect the assumption made in Eq. (3.6). Thus Eq. (3.6) is a valid approximation for the temperature range covered in the experiment. The scattering data from the $\phi=0.104$ solutions will be discussed in the following section, in conjunction with the theoretical fits. The experiment finds an increasing ordering of the stars as we move away from Θ temperature, as witnessed by a lowering of the osmotic compressibility and the development of a strong peak in the scattering intensity at some finite value of the scattering vector. Therefore a theoretical approach is called for, which will be able to describe quantitatively the structural characteristics of the solution, by employing an effective pair interaction between the stars. The theory and the comparison with the experiment are described in the following section.

IV. THEORY: A COLLOIDAL APPROACH

In previous work [2] we employed a combination of the Witten-Pincus logarithmic pair potential [3] and a Yukawa form in order to describe the properties of stars in a good solvent. Here, we are dealing with stars in a solvent which induces weak excluded-volume interactions. For this situation, Milner *et al.* have developed a self-consistent field (SCF) approach in order to describe the density profile and free energy of polymers grafted on flat plates [4]. Moreover, the free energy cost (effective interaction) between two such plates being brought close to each other at distances smaller than twice the equilibrium brush extension has been calculated in the same work. Subsequently, Mewis *et al.* extended the approach to spherical particles coated with polymer by employing the Derjaguin approximation [17], and Genz *et al.* used this pair interaction to investigate the applicability of hard-sphere equations of state to polymerically stabilized colloidal suspensions [18]. Here, we will use the pair potential developed by Mewis *et al.* to describe the neutron-scattering data for stars in the vicinity of the Θ point.

Our starting point is the effective pair interaction between flat plates *per unit area* of the plates, $\beta\Phi_{\mathrm{FP}}$ ($\beta\equiv 1/k_BT$), as a function of the interplate separation h which reads as [4]

$$\beta\Phi_{\mathrm{FP}}(h)=\frac{\pi^2}{24}\frac{L^2\sigma}{Nl^2}\left[\frac{2L}{h}-\frac{9}{5}+\left(\frac{h}{2L}\right)^2-\frac{1}{5}\left(\frac{h}{2L}\right)^5\right], \tag{4.1}$$

involving the monomer length l, the number of monomers per chain N, the isolated polymer layer thickness L, and the surface grafting density σ. The above expression is valid for $h<2L$; for larger distances $\beta\Phi_{\mathrm{FP}}(h)$ vanishes.

Let us now assume that such polymeric brushes are grafted on rigid particles having radius a. If two such particles are brought within a center-to-center distance r, the distance between the grafting surfaces is $h=r-2a$. In the Derjaguin approximation [17,18] the pair potential between two such entities is given by

$$\beta V(h)=\pi a\int_h^{2L}\beta\Phi_{\mathrm{FP}}(D)dD, \tag{4.2}$$

which gives, using Eq. (4.1),

$$\beta V(r)=\begin{cases}\infty, & r<2a\\ U_0\left[-\ln y-\frac{9}{5}(1-y)+\frac{1}{3}(1-y^3)-\frac{1}{30}(1-y^6)\right], & 2a<r<2(a+L)\\ 0, & 2(a+L)<r\end{cases} \tag{4.3}$$

where $y=(r-2a)/(2L)$ and the prefactor U_0 is given by

$$U_0=\frac{\pi^3}{12}\frac{L^3a\sigma}{Nl^2}=\frac{\pi^2L^3f}{48Nl^2a}, \tag{4.4}$$

with f denoting the functionality of the stars, i.e., the number of chains attached to the surface. Here, $f=64$.

Since the SCF considerations which lead to the pair interaction given by Eq. (4.3) are valid for stretched chains with weak self-avoidance [4], the above potential is a natural candidate for a colloidal description of stars in the vicinity of the Θ point. According to the ''blob'' picture of Daoud and Cotton [19], a star consists of three regions: an inner ''core,'' where the polymer concentration reaches the value unity and the chains are completely stretched; an intermediate ''unswollen'' region where the behavior of the chains within the blobs is Gaussian; and an outer, ''swollen'' region where the chains show self-avoiding behavior within the blobs. In the vicinity of the Θ point, the outer, swollen region disappears and the chains are locally Gaussian but globally stretched, i.e., the radius of gyration of the whole star behaves as $R_G\approx lN^{1/2}f^{1/4}$, and the additional $f^{1/4}$ factor expresses the stretching of the chains [1,19]. If the chains are short enough so that the stars reduce to their central cores, they never allow any overlap [19]. Hence, it is natural to identify the core of the star with a rigid particle on which f polymeric chains are attached. Then, the parameter a in Eqs. (4.3), (4.4) above can be identified with the core radius. According to the scaling picture [19], the number of monomers in the core, N_c, behaves as $N_c\sim\sqrt{f}$ and hence $a\sim l\sqrt{f}$, since in the core the chains are completely stretched.

Let us now discuss in some detail the determination of the parameters entering the pair potential (4.3), which follows entirely from experimentally measured quantities. The length of a monomer is $l_0=5$ Å and $f=64$. Thus $a\sim 40$ Å. Notice that we differentiate between l_0, the length of a monomer and the parameter l entering in Eq. (4.4). Since the monomers are not really orientationally uncorrelated with one another, the latter should not be the ''bare'' monomer length but it should rather be identified with the persistence length of the isolated chain [20]. Accordingly, we model the chains as Kratky-Porod sequences [20] of monomers. The chemical bonding of polybutadiene is such that each monomer forms a tetrahedral angle $\gamma=109.47°$ with the next one in the chain, thus the acute angle is $\alpha=180°-\gamma=70.53°=1.23$ rad. The persistence length is then [20]

$$l_p\equiv l=\frac{2l_0}{\alpha^2}=6.6\ \text{Å}. \tag{4.5}$$

In addition, the number of monomers N in Eq. (4.3) is, for the same reasons, not the bare number of monomers outside the core, N_0-N_c, but rather a reduced number of orientationally independent subunits resulting from regrouping of the original segments. Forming groups of two monomers brings us already significantly beyond the persistence length;

TABLE III. The parameters used for the potential given by Eq. (4.3) for the fitting of the experimental total scattering intensity: (a) with the choice $a=40$ Å, (b) with the choice $a=50$ Å.

(a)	$a=40$ Å, $l=6.6$ Å, $N=80$		
T (°C)	R_0 (Å)	L (Å)	U_0
40	132	92	73.4
50	138	98	88.9
60	145	105	109.2
70	150	110	125.6
80	155	115	143.6
(b)	$a=50$ Å, $l=6.6$ Å, $N=80$		
T (°C)	R_0 (Å)	L(Å)	U_0
40	132	82	41.6
50	138	88	51.4
60	145	95	64.7
70	150	100	75.5
80	155	105	87.4

thus we choose $N=(N_0-N_c)/2=80$. Finally, we have to determine L, the extent of the polymeric brush beyond the core. Clearly, if R_0 is the corona radius of the star, then $L=R_0-a$. To determine the latter, we use the experimentally measured radius of gyration R_G and hydrodynamic radius R_H of the stars. Indeed, we know [1] that $R_G<R_0<R_H$. Thus we proceed as follows: for the temperature closest to the Θ point of the stars ($T=40$ °C), we use R_0 as a fit parameter in order to obtain good agreement between the experimental and theoretical total scattering intensities. This yields $R_0(T=40\ °\mathrm{C})=128$ Å. For the four remaining temperatures, we scale this number according to the law $R_0(T)=R_0(T=40\ °\mathrm{C})R_G(T)/R_G(T=40\ °\mathrm{C})$, where R_G is always read off from the experimental measurements. This is natural since we expect that the overall radius of the star and its radius of gyration have a fixed ratio at all temperatures in the vicinity of the Θ point.

Since the scaling theory predicts only $a\sim l_0\sqrt{f}$ without the overall coefficient (of order unity) we have used two different choices for this quantity, $a=40$ Å and $a=50$ Å, finding that the resulting fits of the total scattering intensity curves are quite insensitive to this choice. The list of the parameters obtained in the way described above is summarized in Table III. The resulting pair potential is shown in Fig. 5. Notice that the change of the temperature has two effects: on the one hand, the parameters of the potential itself change, thus making it more repulsive as we move away from the Θ point. On the other hand, the average interparticle separation measured in units of R_G (which is the unit of length in Fig. 5), $(\rho R_G^3)^{-1/3}$, becomes smaller as the temperature is raised. Thus the particles find themselves in increasingly repulsive regions of the pair potential and this results in structure factors that develop more and more structure as we move away from the Θ point.

Further evidence for the validity of the procedure described above in order to determine the overall size of the star, i.e., the parameter R_0 of the pair potential, is offered by making a comparison between the second virial coefficient $B_2(T)$ obtained theoretically by employing the pair potential

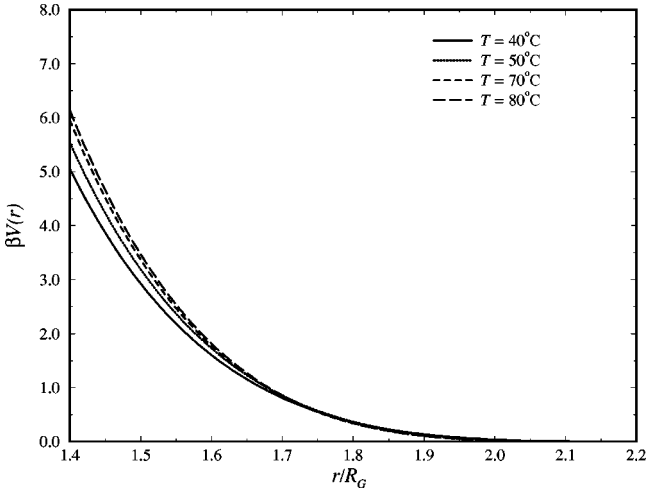

FIG. 5. The pair potential of Eq. (4.3) vs r/R_G. The curve for $T=60$ °C has been omitted since it runs very close to that for $T=70$ °C. Notice that R_G changes with temperature, as shown in Table I. The parameters are listed in Table III(b).

of Eq. (4.3) and that obtained from experiment. The former can be calculated from the formula [21]

$$\overline{B}_2^{\mathrm{thr}}(T)\equiv R_G^{-3}B_2(T)=-2\pi\int_0^\infty x^2\{\exp[-\beta V(x)]-1\}dx, \tag{4.6}$$

where $x=r/R_G$. On the other hand, the corresponding experimental quantity can be calculated from the measured values of $A_2(T)$ according to

$$\overline{B}_2^{\mathrm{expt}}(T)=\frac{R_G^{-3}M_W^2A_2(T)}{N_A}, \tag{4.7}$$

where M_W is the weight-average molar weight of the star, determined by LALLS to be 725 000 g/mol; $A_2(T)$ and R_G can be read off from Table I. In Table IV we show the comparison between $\overline{B}_2^{\mathrm{thr}}(T)$ and $\overline{B}_2^{\mathrm{expt}}(T)$, demonstrating that the two are in very good agreement, within experimental errors.

Using now the pair potential described above and employing the accurate and thermodynamically consistent Rogers-Young closure [22], we have determined the structure factors $S(Q;T)$ for each temperature and for the experimentally measured density ρ. The latter is obtained by the formula $\rho=\phi N_A/V_W$, where $\phi=10.4\%$ and V_W is read off from the third column of Table II. The results are shown in Fig. 6. As can be seen, $S(Q)$ develops more structure as we move away

TABLE IV. Comparison between theoretical and experimental second virial coefficients.

T (°C)	$\overline{B}_2^{\mathrm{thr}}$ ($a=40$ Å)	$\overline{B}_2^{\mathrm{thr}}$ ($a=50$ Å)	$\overline{B}_2^{\mathrm{expt}}$
40	12.15	11.92	9.42 ± 2.30
50	12.49	12.30	14.64 ± 3.20
60	13.13	12.84	14.04 ± 3.41
70	13.14	12.83	13.87 ± 3.12
80	13.43	13.12	13.69 ± 2.85

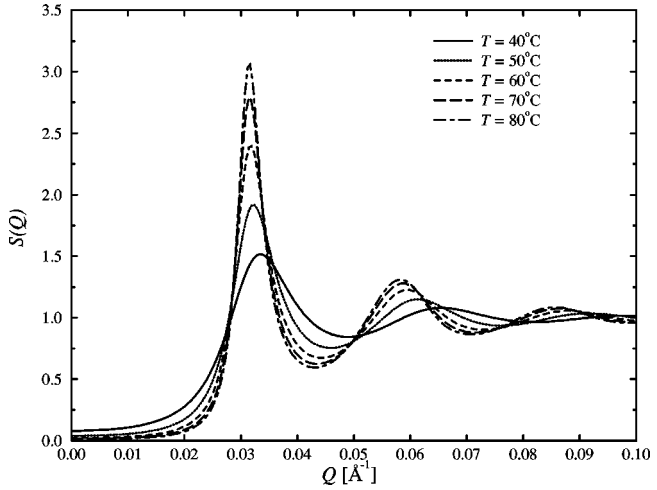

FIG. 6. The bare structure factors $S(Q)$ for the pair potentials of Fig. 5 as obtained from the Rogers-Young closure.

from the Θ point and, in addition, the peak moves to lower values of the scattering vector, in agreement with the experimental observations. Moreover, it can be seen that the solution develops quite strong ordering as we raise the temperature. To make the comparison with experiment quantitative, we must first multiply $S(Q)$ with the form factor according to Eq. (3.6) and then convolute the product with the resolution function $R(Q,Q_0)$ of the experimental apparatus, obtaining the theoretical total scattering intensity:

$$\frac{I_{\mathrm{th}}(Q_0)}{\phi}=\frac{1}{\phi}\frac{N_A}{\Delta\rho^2}\frac{d\Sigma}{d\Omega}(Q_0)$$
$$=[G(Q)S(Q)+F(Q)]*R(Q,Q_0). \qquad (4.8)$$

For the form factor terms $G(Q)$ and $F(Q)$ we use the Beaucage fit [13] with the parameters listed in Table II; the resolution function is given by Eq. (3.5). In Fig. 7 we show the theoretical results for the total scattering intensity in comparison with the experimentally measured values. As can be seen, there is excellent agreement for the temperature closest to the Θ point ($T=40$ °C) and the agreement becomes slightly worse as we move to higher temperatures. In particular, the compressibility [$Q\to 0$ limit of $I(Q)$] predicted by theory is lower than the experimental value. However, the shape of the curve, the height as well as the location of the peak position are always quite satisfactory. There are two possible reasons for the discrepancies: on the one hand, the pair potential of Eq. (4.3) is supposed to work best when the excluded volume interactions are small and the latter increase as we raise the temperature. On the other hand, as the temperature increases and the stars grow in size with the core size being kept fixed, the validity of the underlying Derjaguin approximation becomes questionable. Indeed, the latter is strictly valid when $L \ll a$. Still, the potential incorporates several characteristic features of the supposed ''true'' interaction, e.g., the finite range and the divergence close to the core, and it turns out to provide an overall satisfactory description of the star solution not too far away from the Θ point.

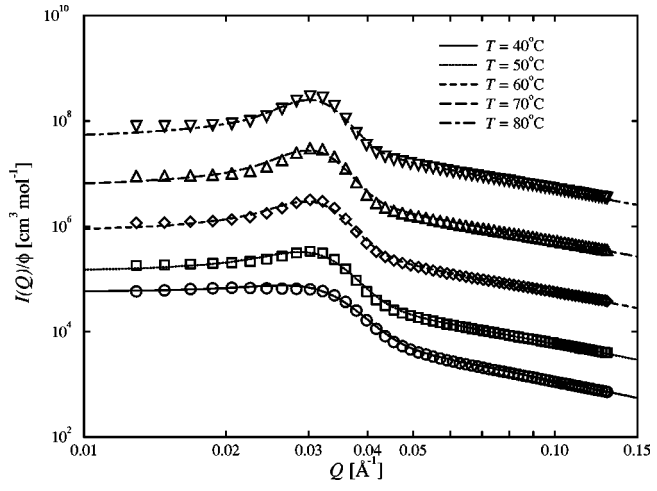

FIG. 7. Theoretical (curves) vs experimental (points) total scattering intensities for stars in the vicinity of the Θ point. The theoretical curves have been obtained by the procedure described in the text using the parameters of Table III(b). For clarity, the data have been multiplied by constants: 50 °C:5, 60 °C:50, 70 °C:500, 80 °C:5000.

V. DISCUSSION AND CONCLUSIONS

The dilute solution properties of the polybutadiene 64-arm star close to the Θ point have been examined by SANS. In the experiment, the Q range was restricted, so that the Guinier range $QR_G \leqslant 1$ was not accessible. Therefore we applied the Berry extrapolation, which is meaningful for an extended Q range up to $QR_G \leqslant 2$ encompassing our lowest Q data.

The values of R_G increase with rising temperature, which was expected and results from the swelling of the star. The values of A_2 reflect the change of the solvent quality from nearly that of a Θ solvent at 40 °C to a better quality at 80 °C. The parameter d_f is determined from the scattering at high Q values. Its relation to the Flory exponent ν is given by the simple equation

$$d_f=\frac{1}{\nu}. \qquad (5.1)$$

The values obtained for ν are in the range between 0.55 and 0.64, and indicate that the quality of the solvent changes in the temperature range from nearly Θ-like to a better quality. Since in the case of star polymers coherency effects arising from the superposition between different blobs influence the scattering behavior [1] in the low Q range, a good solvent quality for stars is related to ν values around 0.67. Thus, in this experiment, a good solvent quality was not yet reached.

Another similar and often applied expression [1,16,23] for the form factor of stars, developed by Dozier *et al.* [24], was also used to fit the experimental data. In this model, the form factor comprises again two different terms, $G_D(Q)$ and $F_D(Q)$, where $G_D(Q)=V_W\exp[-(Q^2R_G^2/3)]$ is the Guinier exponential and $F_D(Q)$ is expressed by the Fourier transform of the mass-mass correlation function of a swollen polymer coil $g(r)$, where the blob dimension enters as a screening length ξ:

$$g(r)\sim r^{1/\nu-3}\exp(-r/\xi). \qquad (5.2)$$

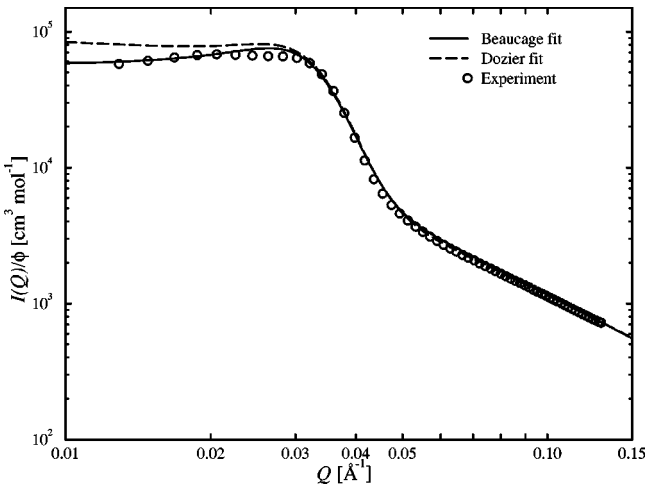

FIG. 8. Comparison of the theoretical total scattering intensities at $T=40$ °C obtained with the Beaucage (solid line) and the Dozier fit (broken line). The symbols denote experimental data. Notice the overestimation of the compressibility obtained by the Dozier fit.

The transformation leads to the following expression for $F_D(Q)$:

$$F_D(Q)=\frac{4\pi\alpha}{Q\xi}\frac{\sin[\mu\ \tan^{-1}(Q\xi)]}{[1+Q^2\xi^2]^{\mu/2}}\Gamma(\mu), \qquad (5.3)$$

where $\mu=1/\nu-1$ and $\Gamma(\mu)$ is the gamma function; α denotes a normalization constant, which is an adjustable parameter as well as V_W, R_G, and ν. It can be seen from Eq. (5.3) that $F_D(Q)$ does not vanish in the limit of $Q\rightarrow 0$ and thereby contributes to the forward scattering and to V_W, which is already completely described by the first term $G_D(Q)$. Thus the molecular volume is underestimated in this model and can only be determined correctly if the condition $G(0)S(0)\gg F(0)$ is fulfilled. Regarding the single star form factor, this condition is fulfilled, while in the case of the semidilute solution it is not valid any more, because the forward scattering intensity is rather low. Thus, although fits applying the Dozier model led to an excellent agreement between experimental results and theory for the pure form factors, this model could not be applied to the rather concentrated solutions, since the forward scattering intensity, i.e., the osmotic compressibility, was always overestimated. This effect is shown in Fig. 8, where the theoretical calculations based on the Dozier model and the Beaucage model are compared with the experimental data at 40 °C.

It has been shown theoretically [25] and experimentally [26,27] that branching causes a lowering of the Θ temperature of a polymer. Results from former light-scattering experiments revealed only a negligible effect in the system polybutadiene-protonated 1,4-dioxane [6]. The Θ temperature of linear and star polybutadienes was reported to be close to 26.5 °C. Also the change from protonated to deuterated solvent can influence the Θ temperature of a polymer-solvent system. Experimentally it was found that such a change in the system causes a shift in Θ temperature to higher values. Thereby, differences between the Θ temperatures in the range of 2 °C have been observed [28] for the system polybutadiene-biphenyl. In the case of the system under investigation, a Θ temperature of 31 °C was determined, yielding an increase of 5 °C in comparison to the protonated solvent. Thus the effect on deuteration overcompensates the lowering of the Θ temperature by branching and is in this case relatively high in comparison to other systems [28].

The theoretical investigations for the description of the scattering intensity curves of stars in the vicinity of the Θ point revealed that the pair interaction which has to be employed is quite different from that for stars in a good solvent [2]. Indeed, if we applied the logarithmic Yukawa potential of Ref. [2] to this case, we would find that the solutions ought to be actually crystalline, i.e., that potential is too repulsive. This is expected, since the low quality of the solvent induces weaker repulsions between stars than a good solvent. Thus, although the Θ point is an unstable fixed point in the renormalization group sense and therefore the universal properties of very long chains slightly away from the Θ temperature are identical to those of chains in good solvents, we find that for nonuniversal quantities the vicinity of the Θ point matters. At this stage, we have been able to describe in a satisfactory way star solutions in good solvents on the one hand and in Θ-like solvents on the other, by employing different effective pairwise interactions for each case. Although the two interactions have some superficial similarities (e.g., the logarithmic term for close approaches), the arguments that lead to them are quite different for each case. Thus the development of a unified theoretical approach which would apply for the whole range of solvent quality, i.e., going from Θ-like to a good solvent and which thus would bridge the gap between the two borderline cases, remains a problem for the future.

ACKNOWLEDGMENT

We wish to thank Professor E. Eisenriegler for helpful discussions.

[1] G. S. Grest, L. J. Fetters, J. S. Huang, and D. Richter, Adv. Chem. Phys. **XCIV**, 67 (1996).

[2] C. N. Likos, H. Löwen, M. Watzlawek, B. Abbas, O. Jucknischke, J. Allgaier, and D. Richter, Phys. Rev. Lett. **80**, 4450 (1998).

[3] T. A. Witten and P. Pincus, Macromolecules **19**, 2509 (1986).

[4] S. T. Milner, T. A. Witten, and M. E. Cates, Macromolecules **21**, 2610 (1988).

[5] L.-L. Zhou and J. Roovers, Macromolecules **26**, 963 (1993).

[6] J. Roovers, L.-L. Zhou, P. M. Toporowski, M. v. d. Zwan, H. Iatrou, and N. Hadjichristidis, Macromolecules **26**, 4324 (1993).

[7] J. M. Carella, W. W. Graessley, and L. J. Fetters, Macromolecules **17**, 2775 (1984).
[8] U. Grigull, *Wärme- und Stoffübertragung*, 1st ed. (Springer, Berlin, 1989).
[9] T. P. Russel, J. S. Lin, S. Spooner, and G. D. Wignall, J. Appl. Crystallogr. **21**, 629 (1988).
[10] G. C. Berry, J. Chem. Phys. **44**, 4550 (1966).
[11] M. Daoud and G. Jannink, J. Phys. (France) **37**, 973 (1976).
[12] G. Beaucage, J. Appl. Crystallogr. **28**, 717 (1995).
[13] G. Beaucage, J. Appl. Crystallogr. **29**, 134 (1996).
[14] J. S. Pedersen, D. Posselt, and K. Mortensen, J. Appl. Crystallogr. **23**, 321 (1990).
[15] H. Benoit, J. Polym. Sci. **11**, 507 (1953).
[16] L. Willner, O. Jucknischke, D. Richter, J. Roovers, L.-L. Zhou, P. M. Toporowski, L. J. Fetters, J. S. Huang, M. Y. Lin, and N. Hadjichristidis, Macromolecules **27**, 3821 (1994).
[17] J. Mewis, W. J. Frith, T. A. Strivens, and W. B. Russel, AIChE. J. **35**, 415 (1989).
[18] U. Genz, B. D'Aguanno, J. Mewis, and R. Klein, Langmuir **10**, 2206 (1994).
[19] M. Daoud and J. P. Cotton, J. Phys. (France) **43**, 531 (1982).
[20] J. des Cloiseaux and G. Jannink, *Les Polymères en Solution* (Les Éditions de Physique, Les Ulis, 1987).
[21] J. P. Hansen and I. R. McDonald, *Theory of Simple Liquids*, 2nd ed. (Academic, London, 1986).
[22] F. A. Rogers and D. A. Young, Phys. Rev. A **30**, 999 (1984).
[23] L. Willner, O. Jucknischke, D. Richter, B. Farago, L. J. Fetters, and J. S. Huang, Europhys. Lett. **19**, 297 (1992).
[24] W. D. Dozier, J. S. Huang, and L. J. Fetters, Macromolecules **24**, 2810 (1991).
[25] F. Candau, P. Rempp, and H. Benoit, Macromolecules **5**, 627 (1972).
[26] B. J. Bauer, N. Hadjichristidis, L. J. Fetters, and J. Roovers, J. Am. Chem. Soc. **102**, 2410 (1980).
[27] J. Roovers and S. Bywater, Macromolecules **7**, 443 (1974).
[28] A. T. Boothroyd, G. L. Squires, L. J. Fetters, A. R. Rennie, J. C. Horton, and A. M. B. G. de Vallêra, Macromolecules **22**, 3130 (1989).